

Article

Performance Analysis of Power Allocation and User-Pairing Techniques for MIMO-NOMA in VLC Systems

Hesham S. Ibrahim ^{1,2,*}, Mohamed Abaza ³, Ali Mansour ¹ and Ayman Alfalou ²¹ Lab-STICC, CNRS UMR 6285, ENSTA Bretagne, 2 Rue François Verny, 29806 Brest, France; mansour@ieee.org² LSL Teams, L@b ISEN, Yncrea Ouest, 20 Rue Cuirasse Bretagne, 29200 Brest, France; ayman.al-falou@isen-ouest.yncrea.fr³ Arab Academy for Science, Technology and Maritime Transport, Giza 2033, Egypt; mohamed.abaza@aast.edu

* Correspondence: hesham.sadat@ensta-bretagne.org

Abstract: In this paper, we evaluate the performance of multiple-input multiple-output (MIMO) communication systems applied with a non-orthogonal multiple access (NOMA)-based indoor visible light communication (VLC). We present two efficient user-pairing algorithms for NOMA in VLC, aiming to enhance achievable data rates effectively. Our investigation involves the application of three low-complexity power allocation techniques. Comparative analysis reveals performance enhancements when employing the proposed schemes, especially when contrasted with NOMA without user pairing and orthogonal frequency division multiple access (OFDMA). Additionally, we explore the performance of both algorithms in scenarios with both even and odd numbers of users. Simulation results demonstrate the superiority of NOMA in comparison to OFDMA.

Keywords: non-orthogonal multiple access (NOMA); visible light communication (VLC); multiple-input multiple-output (MIMO); fixed power allocation (FPA); gain ratio power allocation (GRPA); normalized gain difference power allocation (NGDPA); next-largest-difference user-pairing algorithm (NLUPA); uniform channel gain difference pairing algorithm (UCGD)



Citation: Ibrahim, H.S.; Abaza, M.; Mansour, A.; Alfalou, A. Performance Analysis of Power Allocation and User-Pairing Techniques for MIMO-NOMA in VLC Systems.

Photonics **2024**, *11*, 206. <https://doi.org/10.3390/photonics11030206>

Received: 3 January 2024

Revised: 2 February 2024

Accepted: 23 February 2024

Published: 25 February 2024



Copyright: © 2024 by the authors. Licensee MDPI, Basel, Switzerland. This article is an open access article distributed under the terms and conditions of the Creative Commons Attribution (CC BY) license (<https://creativecommons.org/licenses/by/4.0/>).

1. Introduction

With the rapid proliferation of smart devices due to the introduction of the Internet of Things (IoT), visible light communication (VLC) has evolved dramatically as a potential solution to the wireless data explosion challenge [1]. Recently, VLC has gained much attention as an effective technology for wireless communication in indoor environments as it exploits the lighting infrastructure, light-emitting diodes (LEDs), to provide high data-rate transmission as well as illumination [2,3]. Furthermore, VLC has several advantages including high security, huge unregulated bandwidth (400–789 THz), high energy efficiency, low cost and high electromagnetic interference immunity [4]. Despite the tremendous bandwidth of VLC, the limited modulation bandwidth of LEDs (few MHz) limits the full exploitation of VLC potential [5]. In order to effectively overcome this challenge, the application of multiple-input multiple-output (MIMO) and advanced multiple access techniques are proposed [6,7].

Implementing MIMO techniques in VLC systems can significantly enhance the system's capacity and provide adequate indoor illumination using multiple LEDs. Additionally, the application of advanced multiple access schemes, including orthogonal frequency division multiple access (OFDMA) and non-orthogonal multiple access (NOMA), further contributes to improving the overall performance of VLC systems [8]. Unlike OFDMA, in which all users have a consistent transmitted power level and divide the available frequency subcarriers, power domain NOMA allocates a specific power level to each user while making the entire bandwidth accessible to all users [9]. In NOMA, variable power levels are assigned to individual users based on their channel gains. This allocation is achieved through a process involving superposition coding (SC) at the transmitters, and successive

interference cancellation (SIC) is employed at the receivers [10]. Studies have shown that NOMA, which is commonly employed for the multiplexing of a limited number of users, aligns with VLC networks that utilize LEDs as compact cells for serving a small number of users. Moreover, NOMA exhibits superior performance in scenarios characterized by high signal-to-noise ratios (SNRs), which is the case in the small cell VLC networks that provide robust line-of-sight (LOS) connections attributed to short transmission distances [11].

Motivated by this, the performance of NOMA-VLC systems is a topic of a lot of research interest [12]. In [13], a VLC system based on MIMO-NOMA was experimentally validated, although power allocation was not taken into account. It is worth mentioning that power allocation plays an important role in NOMA performance. In [14], an optimal power allocation technique based on multi-factor control with a relatively high level of computational complexity called MFOPA was proposed to maximize the total system capacity. Gain ratio power allocation (GRPA) was introduced as an efficient power allocation technique aimed at improving the throughput and user fairness of the VLC system [15]. In [16], the authors suggested a low-complexity power allocation technique called normalized gain difference power allocation (NGDPA), which demonstrates superior performance in terms of the sum rate within MIMO-NOMA-VLC systems when compared to GRPA. In [4], fixed power allocation (FPA) was introduced as a straightforward allocation method that can achieve, in a 2×2 NOMA-MIMO-VLC system, a higher achievable sum rate compared to NGDPA.

Implementing NOMA for all users may not be viable due to the escalating computational complexity associated with SIC as the number of users increases, which leads to decoding delay, SINR deterioration due to SIC error propagation and a high bit error rate. To address this challenge, user pairing is suggested for reducing SIC decoding complexity [10]. An optimal user pairing algorithm was introduced in [17] to maximize the system throughput, and a closed-form global optimal solution for general NOMA networks was derived. The authors of [18] introduced the bipartite matching-based user-pairing (BMUP) algorithm aimed at finding the optimal user grouping solution to minimize the outage probability in hybrid VLC-RF systems. The two algorithms mentioned above are only applicable when the number of users is even, which may not align with practical scenarios. In [19], a user-grouping algorithm employing a genetic algorithm was proposed to maximize the system's total throughput for odd and even numbers of users. Nevertheless, it is important to note that a genetic algorithm may become trapped in a local optimal. On the other hand, there are different simple user-pairing algorithms proposed such as the next-largest-difference user-pairing algorithm (NLUPA) [20] and a uniform channel gain difference (UCGD) pairing algorithm [21].

To this end, it becomes vital, for the practical implementation of NOMA-VLC systems, to apply efficient power allocation schemes with low computational complexity. Furthermore, the combination of suitable power allocation techniques and simple user-pairing strategies can significantly enhance the performance of NOMA-VLC systems. To the best of our knowledge, this paper is the first to investigate the achievable sum rate performance of NOMA-MIMO-VLC systems using different power allocation techniques, including FPA, GRPA and NGDPA, in combination with simple user-pairing algorithms such as NLUPA and UCGD, employing two different strategies. In this context, the users' achievable rate, in scenarios with both even and odd numbers of users, is evaluated through numerical simulations to demonstrate the effect of increasing the number of users. This is in contrast to previous work that focused on system performance with a small number of users. It is noteworthy that while prior studies concentrated on the sum rate performance of the system, our work delves into the achievable rate of individual users to elucidate the characteristics of each power allocation technique and its impact on the user level. Moreover, the performance of the proposed techniques is compared with that of NOMA without user pairing and OFDMA.

The remainder of this paper is organized as follows: in Section 2, we present an indoor downlink NOMA-MIMO-VLC channel description and explain the system model.

In Section 3, we introduce the power allocation schemes and user-pairing algorithms, followed by numerical results and related discussions in Section 4. Finally, we conclude the paper in Section 5.

2. System and Channel Models

We consider an indoor 2×2 NOMA-MIMO-VLC system of two LED transmitters located on the room's ceiling, similar to our previous work in [4]. These LEDs are used to serve N users, where each user has two photodetectors (PDs) facing the ceiling. Figure 1 shows the downlink 2×2 MIMO-VLC system which utilizes NOMA to serve N users.

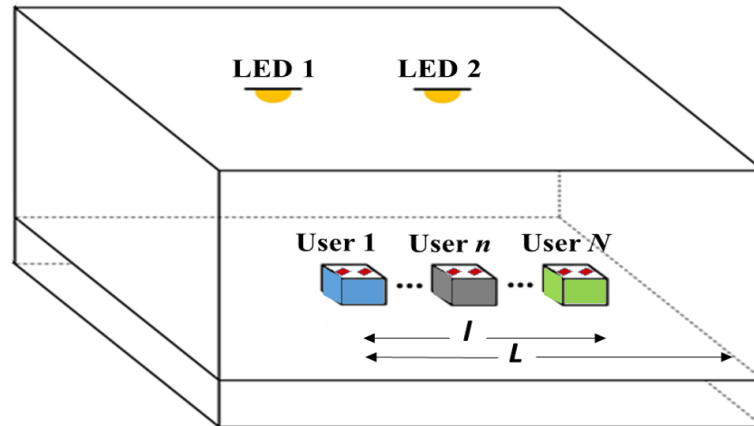


Figure 1. The downlink 2×2 NOMA-MIMO-VLC system serving N users [4].

The VLC channel model in this paper primarily considers the LOS component. While the VLC channel does involve a diffusive part, it is often negligible due to the significantly lower energy of the reflected signal compared to the LOS signal [17]. Figure 2 illustrates how a simple channel model of a single LED serves a user with a single PD. The direct current (DC) channel gain between the j th PD ($j = 1, 2$) of the n th user ($n = 1, \dots, N$) and the i th LED ($i = 1, 2$) can be expressed as provided in [22]:

$$h_{ji,n} = \begin{cases} \frac{A(m+1)}{2\pi d_{ji,n}^2} T_s(\psi_n) g(\psi_n) \cos^m(\phi_n) \cos(\psi_n), & 0 \leq \psi_n \leq \psi_c \\ 0, & \psi_n > \psi_c \end{cases} \quad (1)$$

where A represents the PD's detection area, $m = \frac{-\ln(2)}{\ln(\cos(\Phi_{1/2}))}$ denotes the order of Lambertian emission and $\Phi_{1/2}$ stands for the LED's semi-angle at half power, $d_{ji,n}$ is the distance between the i th LED and the j th PD of the n th user. Field of view (FOV) is denoted by ψ_c , while the angle of incidence and the angle of irradiance are denoted by ψ_n and ϕ_n , respectively. $T_s(\psi_n)$ denotes the gain of the optical filter used at the receiver and $g(\psi_n)$ is the gain of the optical concentrator, which is given by [22]

$$g(\psi_n) = \begin{cases} \frac{n_c^2}{\sin^2(\psi_c)}, & 0 \leq \psi_n \leq \psi_c \\ 0, & \psi_n > \psi_c \end{cases} \quad (2)$$

where n_c represents the corresponding reflective index of the optical concentrator. The noise produced at the PDs follows a Gaussian distribution of zero mean and has the following variance:

$$\sigma_{z_n}^2 = \sigma_{sh_n}^2 + \sigma_{th_n}^2 \quad (3)$$

where $\sigma_{sh_n}^2$ and $\sigma_{th_n}^2$ are the variances of the shot and thermal noises, respectively. The shot noise variance at the n th receiver is given by [23]

$$\sigma_{sh_n}^2 = 2qB(R_p P_{r_n} + I_{bg} I_2) \quad (4)$$

where $q = 1.6 \times 10^{-19}$ Coulombs is electronic charge, R_p is photodetector responsivity, P_{r_n} is the received optical power for the n th user, B is the equivalent bandwidth, I_{bg} is the photocurrent due to background radiation and I_2 is the noise bandwidth factor. Thermal noise is generated within the transimpedance receiver circuit. If the noise effect from the gate leakage current is neglected, thermal variance is represented by [23]

$$\sigma_{th_n}^2 = 8\pi\kappa T_k C_{pd} AB^2 \left(\frac{1}{G_{ol}} I_2 + \frac{2\pi\Gamma}{g_m} C_{pd} AI_3 B \right) \quad (5)$$

which consists of feedback-resistor noise and FET channel noise, where $\kappa = 1.38 \times 10^{-23}$ J/K is the Boltzmann’s constant, T_k is the absolute temperature, G_{ol} is the open-loop voltage gain, C_{pd} is the fixed capacitance of the photodetector per unit area, Γ is the FET channel noise factor, g_m is the FET transconductance and $I_3 = 0.0868$ is a weighting function that depends on the input optical pulse shape [23].

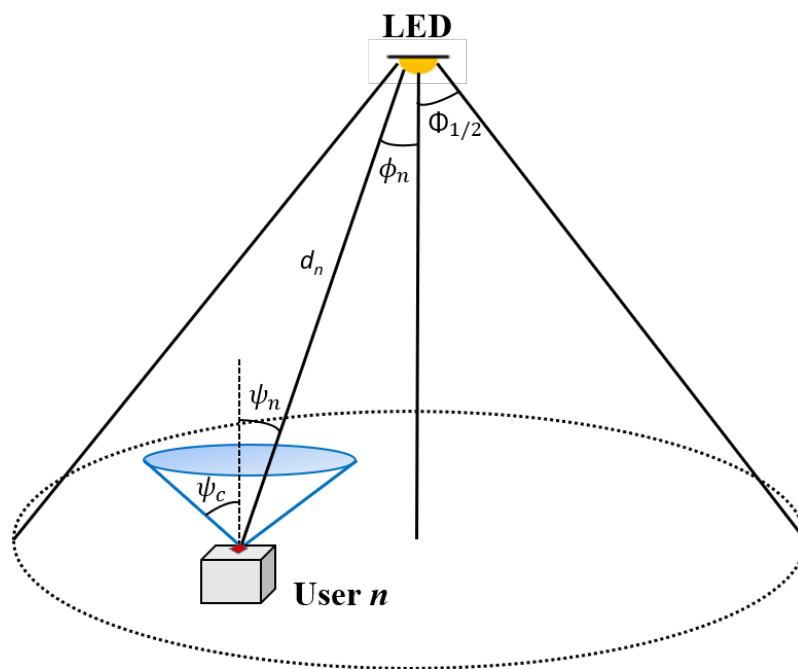


Figure 2. VLC channel model.

Each user may utilize the whole LED’s modulation bandwidth. Additionally, DC-biased optical OFDM (DCO-OFDM) modulation is utilized as the transmitted signal must be real and positive. The 2×2 NOMA-MIMO-VLC system’s schematic using DCO-OFDM is illustrated in Figure 3. The superimposed input signal to the i th LED, following modulation and power domain multiplexing, is expressed as

$$x_i(t) = \sum_{n=1}^N \sqrt{p_{i,n}} s_{i,n}(t) + I_{DC} \quad (6)$$

where $p_{i,n}$ is the electrical power allocated at the i th LED ($i = 1, 2$) for the n th user with overall electrical power $p_{elec} = \sum_{n=1}^N p_{i,n}$, signal $s_{i,n}(t)$ is modulated in the i th LED for the n th user, and I_{DC} stands for the DC bias current provided for each LED. Without any loss of generality, we assume that $p_{elec} = 1$ and N users are ordered based on the sum of their optical channel gains as follows:

$$h_{1i,1} + h_{2i,1} > \dots > h_{1i,n} + h_{2i,n} > \dots > h_{1i,N} + h_{2i,N} \quad (7)$$

The electrical signal received at the n th user is represented as

$$\mathbf{y}_n = R_p \mu P_{op} \mathbf{H}_n \mathbf{x} + \mathbf{z}_n \quad (8)$$

where μ is the modulation index, P_{op} is the LED's output optical power, \mathbf{H}_n is the channel gain matrix relative to the n th user, \mathbf{x} is the transmitted electrical signal vector, \mathbf{z}_n is an additive Gaussian noise vector with zero mean and variance σ_z^2 .

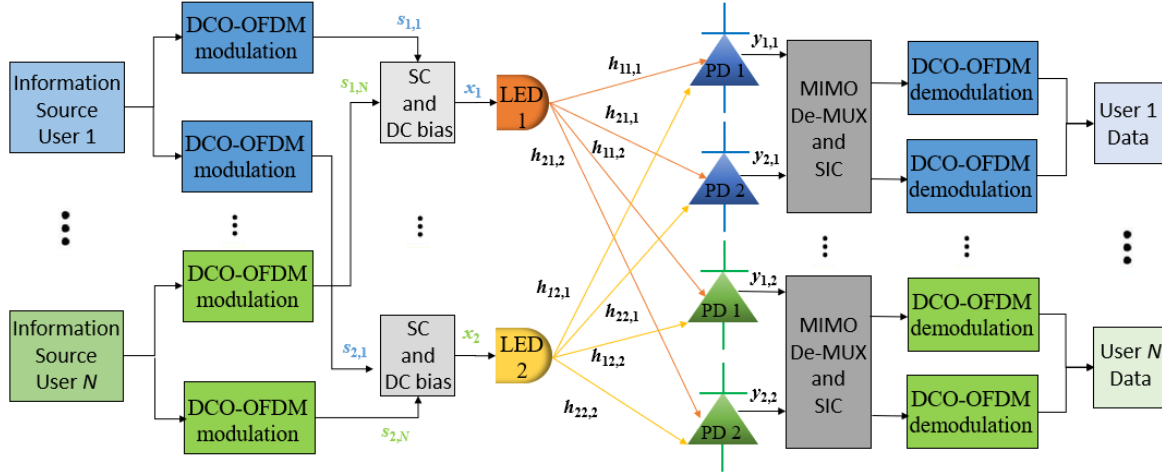


Figure 3. Schematic of a 2×2 NOMA-MIMO-VLC system with N users [4].

To recover the transmitted data, zero-forcing (ZF) MIMO receiver employing basic channel inversion is successfully used [16]. The normalized estimated electrical signal vector obtained by the ZF-based MIMO demultiplexing at the n th user is given by [4]

$$\tilde{\mathbf{x}}_n = \frac{\mathbf{1}}{R_p \mu P_{op}} \mathbf{H}_n^{-1} \mathbf{y}_n = \mathbf{x} + \frac{1}{R_p \mu P_{op}} \mathbf{H}_n^{-1} \mathbf{z}_n \quad (9)$$

To enable SIC at the receiver, the sequence for decoding users concerning the i th LED needs to be established [22]. The decoding order, in relation to the i th LED, is arranged as follows:

$$O_{i,1} < \dots < O_{i,n} < \dots < O_{i,N} \quad (10)$$

When employing SIC at the n th user, message signals directed to users with weaker channel conditions are effectively eliminated. However, the message signal intended for users with stronger channel conditions remains present but is treated as noise in the system [22]. Consequently, the received signal-to-interference plus noise ratio (SINR) received by the n th user from the i th LED can be described as [24]

$$SINR_{i,n} = \frac{(R_p \mu P_{op})^2 p_{i,n}}{(R_p \mu P_{op})^2 \sum_{l=1}^{n-1} p_{i,l} + \gamma_{i,n}^2} \quad (11)$$

where $\gamma_{i,n}$ is the i th element of vector $\boldsymbol{\gamma}_n = \mathbf{H}_n^{-1} \mathbf{z}_n$. The achievable data rate for the n th user is given by [24]

$$R_{i,n} = \begin{cases} \frac{1}{2} B \log_2(1 + SINR_{i,n}), & n = 2, \dots, N \\ \frac{1}{2} B \log_2\left(1 + \frac{(R_p \mu P_{op})^2 p_{i,n}}{\gamma_{i,n}^2}\right), & n = 1 \end{cases} \quad (12)$$

The scaling factor of 1/2 is due to the Hermitian symmetry. We assume that perfect SIC can be performed in the decoding as the n th user can successfully detect the message for the k th user ($n + 1 \leq k \leq N$).

3. Power Allocation Techniques and User-Pairing Algorithms

Efficient power allocation techniques ensure that the available power resources are optimally distributed among users and that can maximize the system's performance. Moreover, user pairing where users are effectively grouped together is essential as it affects how well NOMA can be realized. In this section, we discuss different efficient power allocation techniques and user-pairing algorithms that can improve the system's throughput and fairness.

3.1. Power Allocation Techniques

We depict various low-complexity power allocation methods recognizing their crucial role in enhancing NOMA performance by appropriately assigning power levels to users [2]. Our paper primarily focuses on evaluating, in terms of achievable rates, the performance of NOMA-MIMO-VLC systems using prevalent low-complexity power allocation techniques FPA, GRPA, and NGDPA.

3.1.1. Fixed Power Allocation (FPA)

The FPA is a simple approach that allocates power levels to users based on their order of decoding, regardless of their channel gain values [2]. The electrical power assigned at the i th LED to users n and $n + 1$ is represented by

$$p_{i,n} = \alpha_{i,n} p_{i,n+1} \tag{13}$$

where $\alpha_{i,n}$ is the power allocation factor ($0 < \alpha_{i,n} < 1$).

3.1.2. Gain Ratio Power Allocation (GRPA)

GRPA was introduced in [15] as an effective power allocation technique for NOMA-VLC systems. The power assigned in GRPA depends on the channel gain ratio. However, the GRPA equation in [15] is modified to be suitable for 2×2 NOMA-MIMO-VLC systems with decoding order in (10) where the electrical power assigned to users n and $n + 1$ at the i th LED is given by [15]

$$p_{i,n} = \left(\frac{h_{1i,n+1} + h_{2i,n+1}}{h_{1i,1} + h_{2i,1}} \right)^{n+1} p_{i,n+1} \tag{14}$$

3.1.3. Normalized Gain Difference Power Allocation (NGDPA)

NGDPA was suggested for enhancing the achievable data rate of NOMA-MIMO-VLC systems [16]. Assigning power in NGDPA depends on channel gain difference where the electrical power assigned at the i th LED to n and $n + 1$ users is represented as [16]

$$p_{i,n} = \left(\frac{h_{1i,1} + h_{2i,1} - h_{1i,n+1} - h_{2i,n+1}}{h_{1i,1} + h_{2i,1}} \right)^n p_{i,n+1} \tag{15}$$

3.2. User-Pairing Algorithms

The user pairing concept has been proposed to group users into multiple pairs with the aim of maximizing the channel gain difference among users, thereby enhancing the performance of NOMA. A hybrid NOMA and orthogonal multiple access (OMA) scheme can be employed to accommodate multiple user pairs effectively. To clarify, NOMA is used for the two users within each user pair, while OMA is applied for different user pairs. Hereinafter, we explore two distinct user-pairing algorithms designed to efficiently group N users into $N/2$ pairs. Furthermore, we study the performance of both algorithms in even and odd numbers of user scenarios.

3.2.1. Even Number of Users

Both algorithms, UCGD and NLUPA, adopt identical approaches for user grouping when the number of users is even. This process commences with the users being initially arranged in ascending order according to their individual channel gains. Subsequently, the users are categorized into two groups denoted as g_1 and g_2 which have users with high channel gains and low channel gains, respectively. Group g_1 encompasses the first half of the users who are sorted, commencing from U_1 to $U_{N/2}$, while group g_2 includes the second half of users, commencing from $U_{(N/2)+1}$ to U_N . The aim of the UCGD algorithm is to achieve an almost uniform channel gain difference between in-pair users of all pairs. To facilitate user pairing, one user is chosen from each group, and they are paired together. Therefore, pairing using the UCGD algorithm can be performed as $\mathcal{U}_{i,m} = \{g_{i,1}(m), g_{i,2}(m)\}$, i.e., the m th user pair $\mathcal{U}_{i,m}$ for the i th LED have the m th user in both g_1 and g_2 with $1 \leq m \leq N/2$. On the other hand, the user with the highest channel gain is paired with the user with the lowest channel gain to achieve maximum channel gain difference within paired users in NLUPA. By following the same pattern, user pairing can be accomplished in the following manner: $\mathcal{U}_{i,m} = \{g_{i,1}(m), g_{i,2}((N/2) + 1 - m)\}$. However, the users with medium channel gains are paired with each other, which leads to lesser channel gain difference.

3.2.2. Odd Number of Users

When the number of users is odd, N , after sorting the users in ascending order according to their channel gains, the users are categorized into three groups. The first group g_1 consists of users ranging from U_1 to $U_{((N+1)/2)-1}$, g_2 includes users from $U_{((N+1)/2)+1}$ to U_N , and g_3 contains $U_{((N+1)/2)}$, the middle user. Two strategies can be adopted for user pairing in the case of an odd number of users for both NLUPA and UCGD algorithms. These strategies are illustrated using NLUPA as follows:

- First Strategy: Considers that all users have to be paired. The first pair consists of three users: $g_{i,1}(1)$, $g_{i,2}((N - 1)/2)$ and $g_{i,3}(1)$, which correspond to the first user from group g_1 (nearest to the LED), the last user from group g_2 (farthest from the LED) and the middle user from group g_3 , respectively.
- Second Strategy: Employs a different pairing approach in which the middle user is left unpaired, while the remaining users are paired in the same manner as NLUPA with an even number of users.

Figure 4 demonstrates the user grouping and pairing for even and odd numbers of users using NLUPA and UCGD. Moreover, an identical bandwidth allocation is assessed for different user pairs, in all scenarios equal to $\frac{B}{N/2}$ for an even number of users and $\frac{B}{(N/2)+1}$ for an odd number of users.

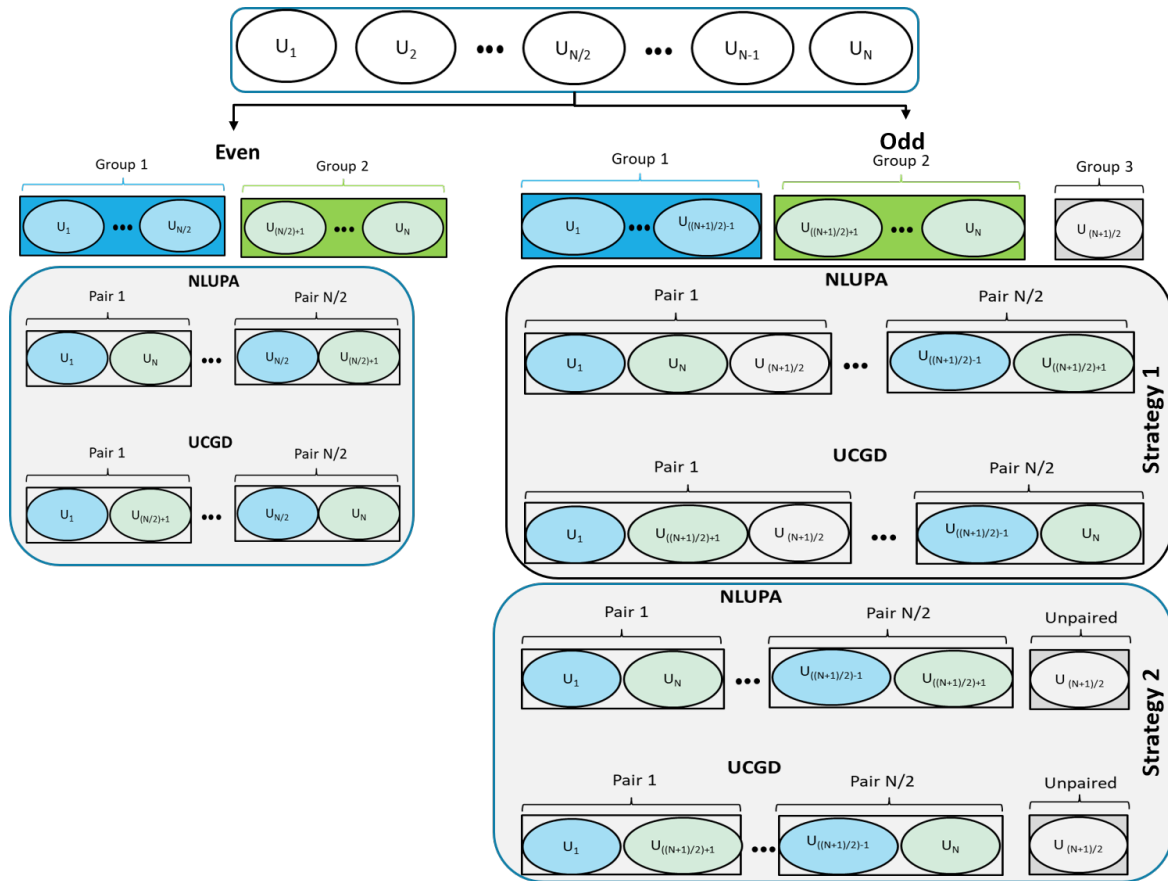


Figure 4. Illustration of user grouping and pairing for even and odd number of users using NLUPA and UCGD.

4. Simulation Results and Discussions

This section investigates the performance of an indoor 2×2 NOMA-MIMO-VLC system employing three power allocation schemes and two user-pairing algorithms through numerical simulations. We chose not to employ any optimization technique in this paper to investigate and maintain a low-computational-complexity system suitable for the practical implementation of NOMA-VLC MIMO. This objective guided our selection of power allocation schemes and user-pairing algorithms. The detailed simulation parameters of the system are shown in Table 1. We analyzed the achievable rate performance using (12) based on the model depicted in Figure 1, where U_1 remains stationary and centered between both LEDs. The distance between U_1 and U_N was denoted by l , while the gap between U_1 and the room's edge was $L = 2$ m. We defined $Q = \frac{l}{L}$ as the normalized offset of U_N with respect to U_1 , whereas $\frac{(n-1)l}{(N-1)L}$ was the normalized offset of U_n relative to U_1 . First, we studied the achievable data rate performance of two users under a perfect SIC, where the power allocation factor, $\alpha_{i,n}$, in (13) was 0.9 to attain the best achievable rate as in [4]. Furthermore, we conducted a performance comparison between OFDMA with a uniform power allocation and NOMA. Finally, to accommodate a greater number of users, we investigated the achievable rate performance of the system using NLUPA and UCGD user-pairing algorithms, comparing their performance for scenarios with both odd and even numbers of users. We chose five users for the odd-numbered scenarios and six users for the even-numbered scenarios as reasonable numbers to compare the performance of the proposed techniques. However, it is important to note that our investigation was not limited to these scenarios, and any number of users can be explored for further analysis.

Table 1. Simulation Parameters.

Description	Symbol	Value
PD detection area	A	1 cm ²
Transmitter semi-angle	$\Phi_{1/2}$	60°
Modulation bandwidth	B	10 MHz
Output optical power	P_{op}	10 W
Responsivity	R_p	0.53 A/W
Optical filter gain	$T_s(\psi_n)$	0.9
Optical concentrator gain	$g(\psi_n)$	2.5
Modulation index	μ	0.5
distance between PDs of each user	d_{pd}	4 cm
Vertical spacing between the users and LEDs	d_{lu}	2.15 m
Spacing between the LEDs	d_l	1 m
FOV of PD	ψ_c	72°

4.1. Two-User Scenario

Initially, we illustrate the achievable rate performance using the three power allocation techniques in two-user scenarios to clarify the specific characteristics of each technique. Figure 5 illustrates the achievable rate for each user for both LEDs versus the normalized offset Q in the 2×2 NOMA-MIMO-VLC system, serving two users ($N = 2$). For LED 1, U_1 represents the nearby user, and U_2 is the far user, as illustrated in Figure 1. In the case of FPA, U_1 achieves a consistently high data rate of 51.2 Mbit/s due to its high SINR according to (12). However, U_2 achieves a constant data rate of 5.2 Mbit/s in the range from $Q = 0.1$ to $Q = 0.7$, which is due to significant interference from U_1 . Then, as U_2 moves farther from the LED, the rate gradually decreases to 1.9 Mbit/s at $Q = 1$ due to the increasing noise, as depicted in Figure 5a. On the other hand, the GRPA strategy aims to achieve fairness among users by initially distributing power almost evenly between them. As U_2 moves farther away from the LED, more power is allocated to the distant user while reducing the power assigned to the nearby user. This explains why the data rate of U_1 decreases from 50.8 Mbit/s to 33.2 Mbit/s as Q increases. Simultaneously, the data rate of U_2 increases in the range from $Q = 0.1$ to $Q = 0.8$, but then decreases as the noise level increases. Conversely, the NGDPA strategy is designed to improve the system’s overall achievable rate. It begins by allocating more power to the far user and less power to the near user. As U_2 moves farther away from the LED, more power is gradually assigned to the near user, eventually reaching 49.8 Mbit/s at the edge of system coverage. Simultaneously, the power allocated to the far user decreases, resulting in a data rate of 2.1 Mbit/s at $Q = 1$. This dynamic allocation of power enhances the total achievable rate of the system. It is important to note that in the context of NOMA, the far user consistently obtains more power than the near user. The distinction between the aforementioned techniques lies in the specific amount of power allocated to each user, but the principle of favoring the far user with higher power remains consistent. In contrast, in the OFDMA scenario, where each user operates in a different frequency subband, the achievable rate of U_1 remains constant at 28.3 Mbit/s, as it has a fixed position. Meanwhile, the rate of U_2 decreases as the normalized offset Q increases, eventually reaching 1.9 Mbit/s at $Q = 1$.

For LED 2, the analysis differs because U_1 is considered the far user and U_2 is the near user in the range from $Q = 0.1$ to $Q = 0.5$, and vice versa in the range from $Q = 0.6$ to $Q = 1$ as shown in Figure 5b. This change in the roles of users affects the interference levels for each user and achievable data rates accordingly. In FPA, U_1 has a fixed low data rate of 5.4 Mbit/s due to the interference from U_2 in the range from $Q = 0.1$ to $Q = 0.5$. Then, the rate suddenly increases to 51.2 Mbit/s and remains fixed from $Q = 0.6$ to $Q = 1$. Meanwhile, U_2 starts with a rate of 51.8 Mbit/s, which gradually decreases due to increasing noise as U_2 moves farther from the LED. When the roles change, and U_2 becomes the far user, the rate drops to 5.4 Mbit/s at $Q = 0.6$ and continues to decrease till 4 Mbit/s at $Q = 1$. The performance of GRPA is quite similar to that of FPA in the range from $Q = 0.1$ to

$Q = 0.5$. However, from $Q = 0.6$ to $Q = 1$, as U_2 moves farther from the LED, the rate of U_1 decreases, while the rate of U_2 increases. This aligns with the concept of GRPA, which aims to enhance the performance of the far user. In the NGDPA scheme, given that U_2 maintains the same channel gain at $Q = 0.1$ and $Q = 0.4$ and U_1 is stationary between both LEDs, the achievable rates are equal in these specified positions. However, there is a slight degradation in U_2 's rate as its SINR decreases with increasing distance from the LED. The same scenario applies to the $Q = 0.2$ and $Q = 0.3$. At $Q = 0.5$, both users have identical channel gains. Following Equation (15), this implies that all the power is allocated to U_2 , leaving U_1 with no power allocation. Consequently, U_1 's rate becomes zero. Starting from $Q = 0.6$, the power allocation pattern shifts, with more power being assigned to the near user (U_2) and less power to the far user (U_1). This results in U_1 achieving 44.9 Mbit/s and U_2 achieving 7.7 Mbit/s at the end of system coverage. It can be seen that the OFDMA performance for U_1 is consistent with what was discussed for LED 1, with no significant changes. However, there is an improvement in U_2 's performance because it is always closer to LED 2 than to LED 1.

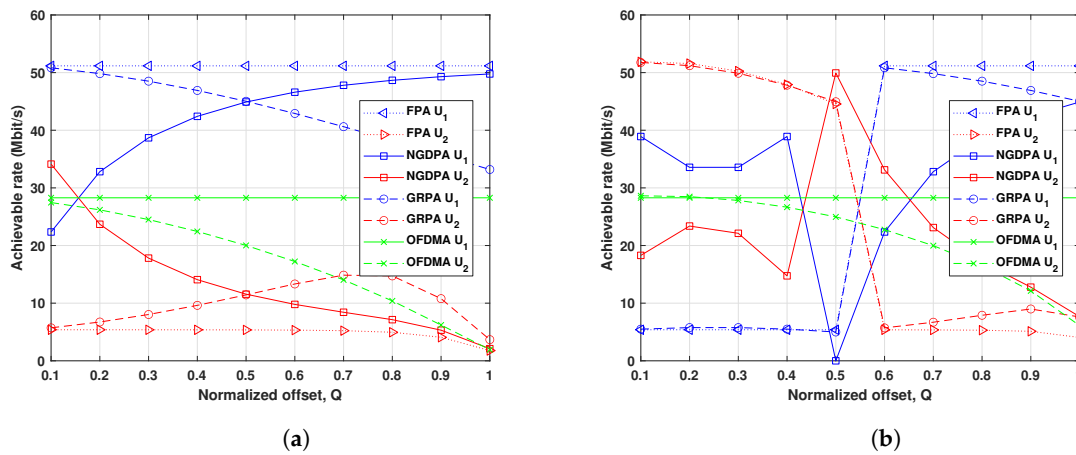


Figure 5. Achievable rate vs. normalized offset-based NOMA and OFDMA with two users ($N = 2$) (a) LED 1 (b) LED 2.

It is worth noting that despite NGDPA achieving a better sum rate than GRPA when aggregating the rates of the users, as demonstrated in [16], in scenarios where both users have the same channel gain, NGDPA performs worse. Furthermore, when the users move far from the LED, NGDPA relies on increasing the power to the near user to achieve a high system sum rate. However, this increase in power allocation to the near user may not be necessary for decoding its data and comes at the expense of the far user. Furthermore, even a simpler technique, FPA, can achieve a better sum rate than NGDPA, as demonstrated in [4].

4.2. Five-User Scenario

We initially evaluate the achievable rates of five users utilizing NOMA with FPA, GRPA, and NGDPA without user pairing, as illustrated in Figure 6. In Figure 6a–c, the achievable rates of LED 1 are depicted, with U_1 to U_5 representing the order of users from the nearest to the farthest.

In the case of FPA, despite U_1 having the lowest assigned power, it attains the highest rate of 43.4 Mbit/s due to the absence of interference from other users. The rates of the remaining users follow their order, with U_5 experiencing the lowest rate of 2 Mbit/s, showing degradation at the end of the coverage area due to elevated noise levels, as depicted in Figure 6a. Meanwhile, the achievable rate of U_1 reduces while the rates of the other users increase as they move away from the LED, as GRPA assigns more power for the far users as Q increases. In contrast, NGDPA, at low Q values, allocates high power to far users U_4 and U_5 and very low power to near users U_1 and U_2 . As Q increases,

NGDPA reduces the power assigned to far users and increases the power assigned to near users. Consequently, the rate of far users decreases due to power reduction and increased interference from near users. The impact on U_1 is relatively slight, given its initial low power, while U_2 achieves a higher rate with increasing Q . The rate of U_3 , the middle user, increases at low Q and then decreases as interference, particularly from U_2 , rises. In Figure 6d–f, the achievable rates of LED 2 are illustrated, featuring a distinct order of users based on the value of Q . The same concept employed for LED 1 in FPA is also applied for LED 2, where the achievable rates of users follow their order, with the highest rate for the nearest user and the lowest for the farthest. Furthermore, the performance of GRPA closely aligns with FPA, particularly at low Q values. However, GRPA aims to improve the performance of the far users as Q increases. This behavior is evident starting from $Q = 0.7$ onward, where the rate of U_5 (farthest user) increases, while U_2 's (nearest user) rate decreases after reaching its peak. On the other hand, NGDPA allocates high power to the farthest users at low Q and high power to the nearest users at high Q . For instance, at low Q values, U_1 (farthest user) receives very high power, while other users are allocated very low power, resulting in low interference and consequently high data rates. As the user order changes, the data rate of U_1 decreases to zero at $Q = 0.7$, then rises as U_1 becomes the middle user. It is noteworthy that the utilization of NGDPA may lead certain users to achieve a zero data rate, as it concentrates most of the power on one or a few users, leaving others with insufficient power.

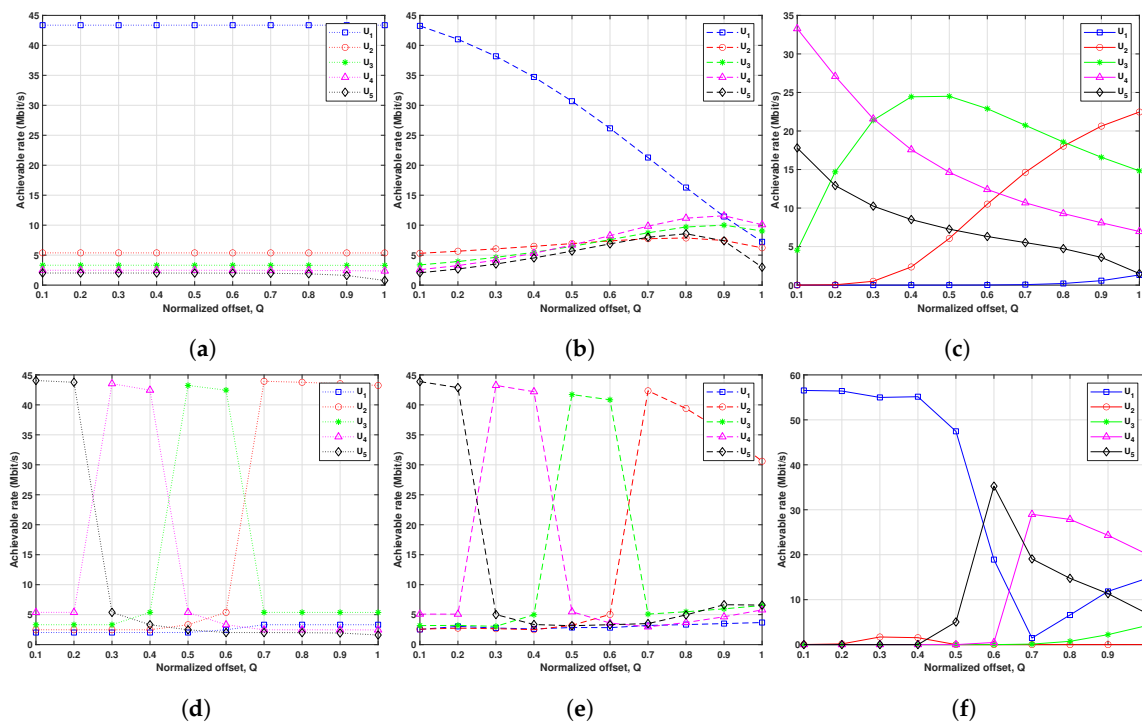


Figure 6. Achievable rate vs. normalized offset-based NOMA with five users ($N = 5$) for LED 1 using (a) fixed power allocation (FPA), (b) gain ratio power allocation (GRPA), (c) normalized gain difference power allocation (NGDPA), and for LED 2 using (d) FPA, (e) GRPA, (f) NGDPA.

In the following analysis, we assess the achievable rates of five users employing NOMA with FPA, GRPA, and NGDPA coupled with NLUPA and UCGD using Strategy 1 user-pairing algorithm, as depicted in Figure 7. Remarkably, for the five-user scenario only, NLUPA and UCGD exhibit identical performance as they share the same pairing strategy. The division of users into two groups proves advantageous, enabling more effective power allocation among users in comparison to the without-grouping scenario. For instance, the performance of U_2 (nearest user in g_2) for LED 1 demonstrates significant data rate improvement with the three power allocation techniques. Furthermore, in NGDPA, the

instances where users achieve zero data rate at different Q values are substantially reduced for both LEDs.

Figure 8 shows the achievable rate performance of five users using NOMA with FPA, GRPA, and NGDPA associated with the NLUPA Strategy 2 user-pairing algorithm. Notably, the performance of the unpaired user (U_3 in LED 1) experiences a significant enhancement as it does not share power with other users. The same pattern is observed in LED 2, although the unpaired user varies based on the user order at each Q value. Moreover, in NGDPA, none of the users attain zero data rate at any Q values for both LEDs. Figure 9 depicts the achievable rate performance of five users using NOMA with FPA, GRPA, and NGDPA associated with UCGD strategy 2 user-pairing algorithm. The performance of FPA aligns with NLUPA Strategy 2, exhibiting consistent results as the pairs change but with identical power distribution. In contrast, GRPA's performance shows slight variations. Remarkably, NGDPA's performance experiences a substantial improvement. It is noteworthy that for both NLUPA and UCGD, Strategy 2 involves fewer applications of SIC compared to Strategy 1. Specifically, Strategy 2 applies SIC $\frac{N-1}{2}$ times, while Strategy 1 applies it $(\frac{N+1}{2}) + 1$ times. On the other hand, both NLUPA and UCGD apply SIC $\frac{N}{2}$ times for an even number of users.

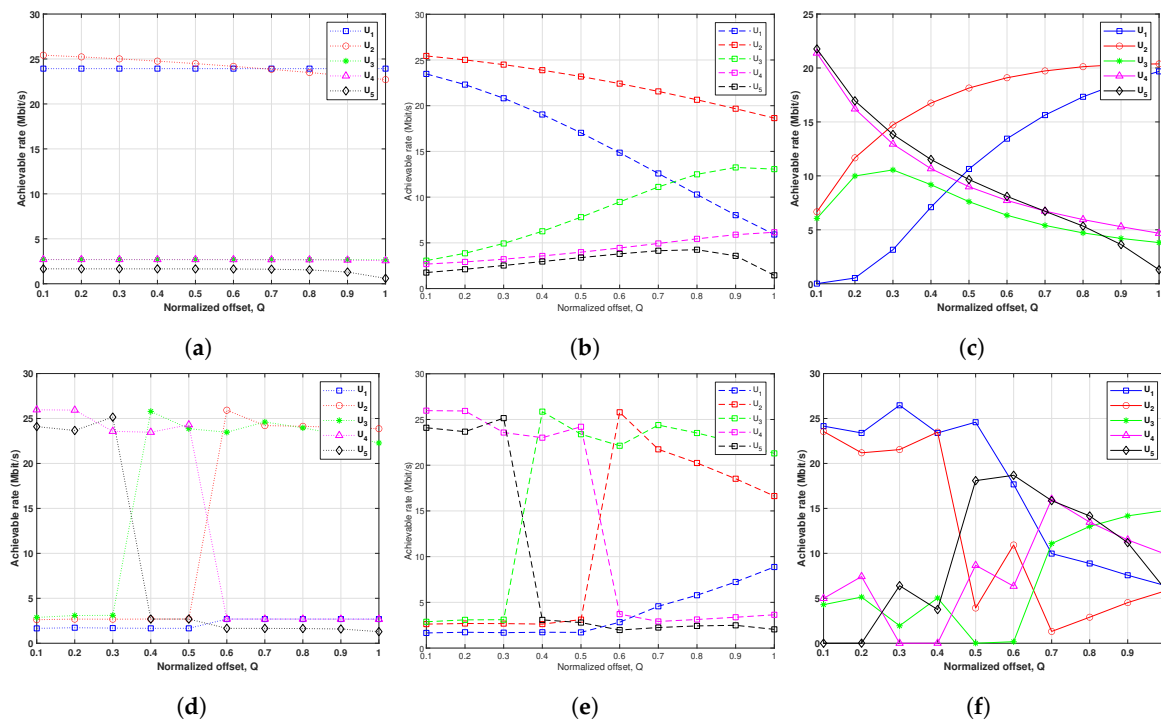


Figure 7. Achievable rate vs. normalized offset-based NOMA with five users ($N = 5$) with Strategy 1 NLUPA/UCGD user pairing of LED 1 using (a) fixed power allocation (FPA), (b) gain ratio power allocation (GRPA), (c) normalized gain difference power allocation (NGDPA), and of LED 2 using (d) FPA, (e) GRPA, (f) NGDPA.

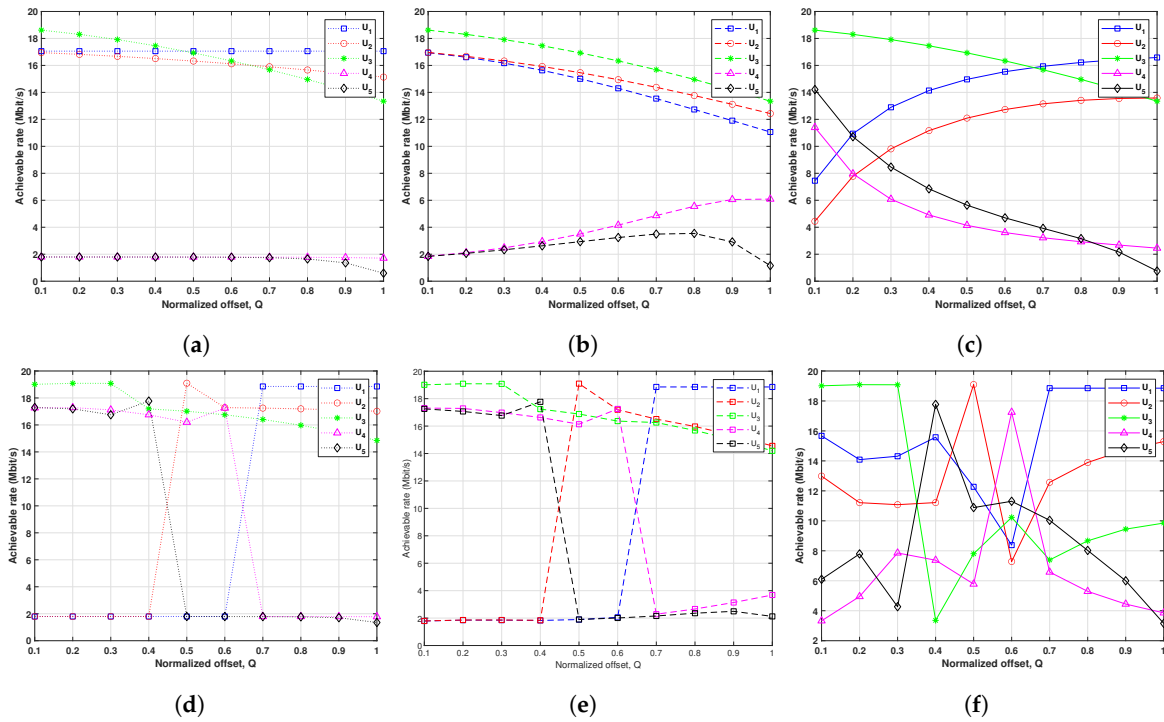


Figure 8. Achievable rate vs. normalized offset-based NOMA with five users ($N = 5$) with Strategy 2 NLUPA user pairing of LED 1 using (a) fixed power allocation (FPA), (b) gain ratio power allocation (GRPA), (c) normalized gain difference power allocation (NGDPA), and of LED 2 using (d) FPA, (e) GRPA, (f) NGDPA.

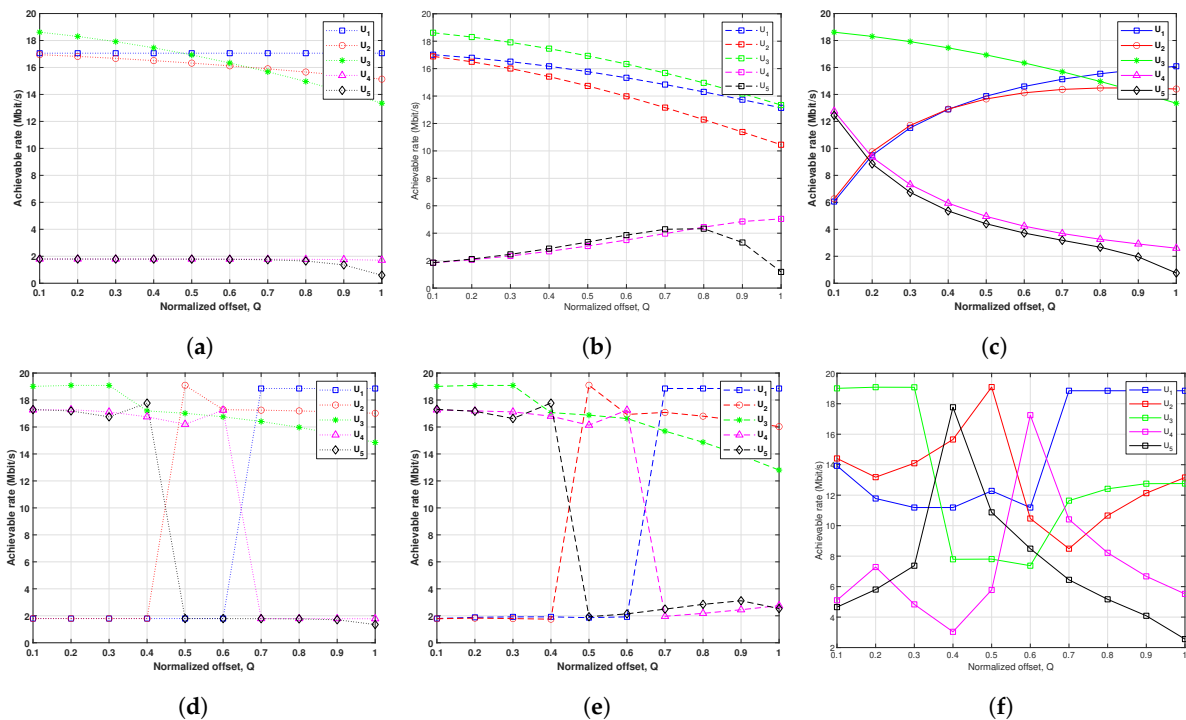


Figure 9. Achievable rate vs. normalized offset-based NOMA with five users ($N = 5$) with Strategy 2 UCGD user pairing of LED 1 using (a) fixed power allocation (FPA), (b) gain ratio power allocation (GRPA), (c) normalized gain difference power allocation (NGDPA), and of LED 2 using (d) FPA, (e) GRPA, (f) NGDPA.

4.3. Six-User Scenario

In this subsection, we present the system’s performance with six users, providing an example of an even number of users. We evaluate the achievable rates of six users utilizing NOMA with FPA, GRPA, and NGDPA without user pairing, as illustrated in Figure 10. The pattern remains consistent with the five-user scenario, where FPA yields data rates in descending order based on the users’ ordering from near to far. However, with GRPA, as Q increases, the achievable rate of the near user decreases, while that of the far users increases. In contrast, NGDPA increases the achievable rate for the near users as Q increases and decreases it for the far users. Moreover, increasing the number of users increases instances of users reaching zero data rate with NGDPA, as observed when comparing the scenarios with five and six users.

In contrast to the case of an odd number of users, all users are paired, eliminating the need for Strategy 1 and Strategy 2 classification. Figure 11 demonstrates the beneficial impact of considering NLUPA user pairing, where pairing the users enhances the achievable rate performance of most users, especially in NGDPA. Figure 12 shows the achievable performance rates of six users using NOMA with FPA, GRPA, and NGDPA combined with the UCGD user-pairing algorithm. UCGD enhances the achievable rate performance compared to NLUPA that has no user with a zero data rate in NGDPA.

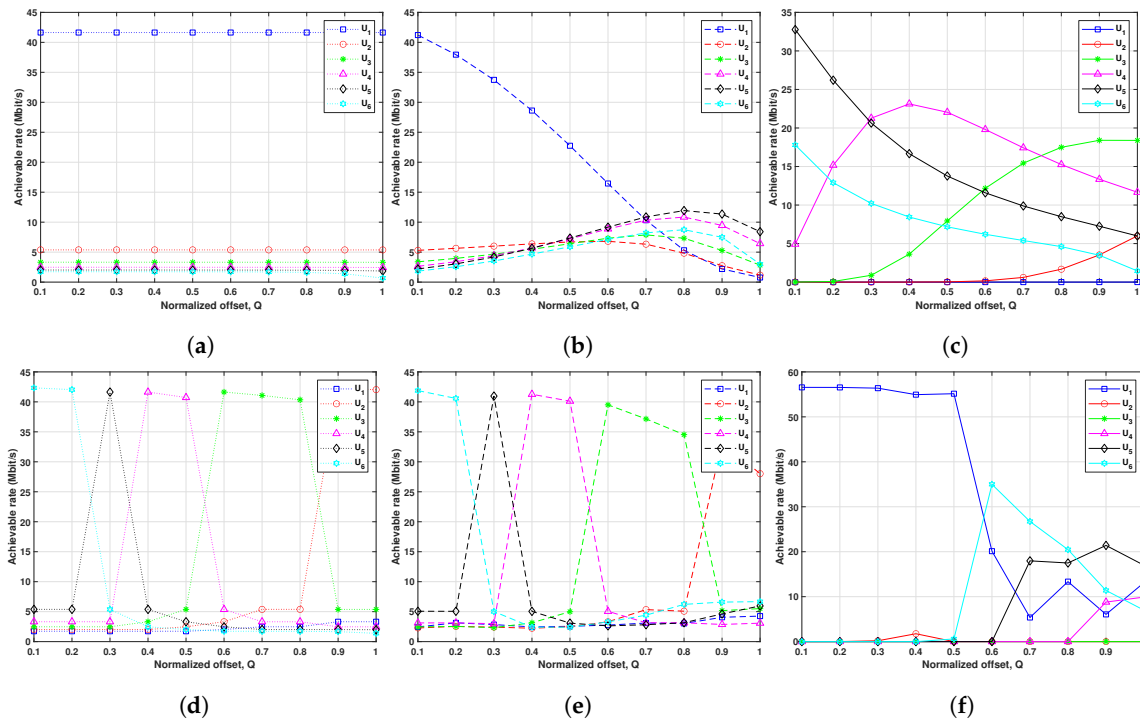


Figure 10. Achievable rate vs. normalized offset-based NOMA with six users ($N = 6$) for LED 1 using (a) fixed power allocation (FPA), (b) gain ratio power allocation (GRPA), (c) normalized gain difference power allocation (NGDPA), and for LED 2 using (d) FPA, (e) GRPA, (f) NGDPA.

4.4. Performance Comparison

For the purpose of a clear comparison between the different power allocation techniques with and without the suggested user-pairing algorithms, we compare the sum rate performance for both five and six users scenarios. The sum rate is the aggregated achievable rate of the users served by both LEDs. Figure 13 illustrates the sum rate for five and six users using OFDMA and NOMA with FPA, GRPA, and NGDPA with and without user-pairing NLUPA and UCGD algorithms.

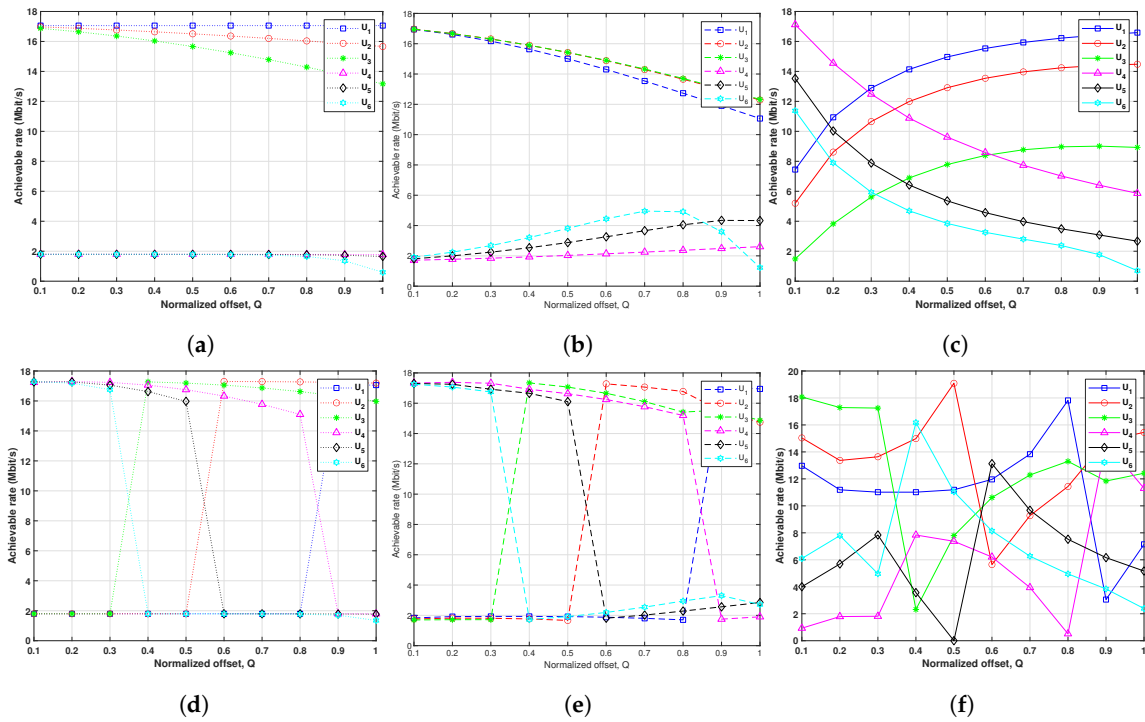


Figure 11. Achievable rate vs. normalized offset-based NOMA with six users ($N = 6$) with NLUPA user-pairing of LED 1 using (a) fixed power allocation (FPA), (b) gain ratio power allocation (GRPA), (c) normalized gain difference power allocation (NGDPA), and of LED 2 using (d) FPA, (e) GRPA, (f) NGDPA.

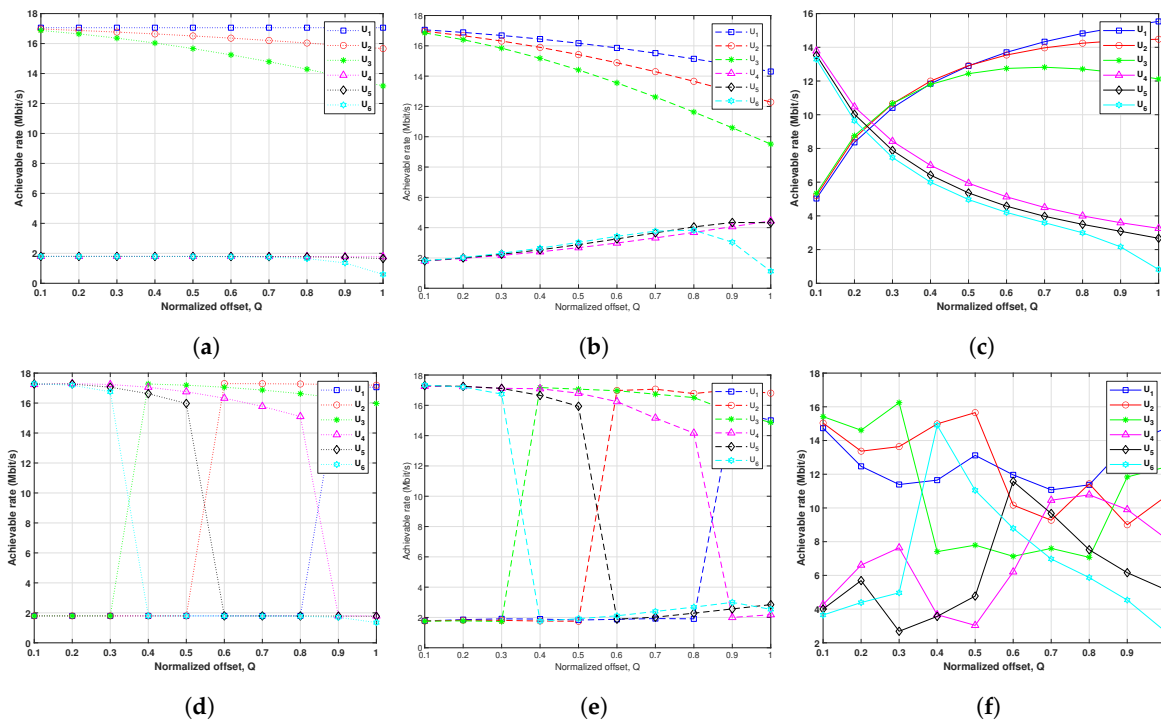


Figure 12. Achievable rate vs. normalized offset-based NOMA with six users ($N = 6$) with UCGD user-pairing of LED 1 using (a) fixed power allocation (FPA), (b) gain ratio power allocation (GRPA), (c) normalized gain difference power allocation (NGDPA), and of LED 2 using (d) FPA, (e) GRPA, (f) NGDPA.

As we can see in Figure 13, OFDMA consistently achieves the lowest sum rate at the system coverage edge compared to NOMA with different power allocation schemes,

except for GRPA in the six-user scenario without grouping. It is crucial to explore the suitable user-pairing algorithm for each power allocation scheme. In the five-user scenario, GRPA achieves a better sum rate using NLUPA Strategy 2, with a marginal difference with NLUPA/UCGD Strategy 1, while NGDPA sees significant improvement using UCGD Strategy 2. On the other hand, FPA without grouping demonstrates the best sum rate performance, primarily contributed by the near user, while grouping allows for other users to achieve better rates. Additionally, in the six-user scenario, GRPA achieves its best sum rate using UCGD, while NGDPA shows substantial improvement using NLUPA. In contrast, FPA, as the five-user scenario, performs optimally without grouping. It is essential to note that while FPA demonstrates the highest sum rate on the system level, it does not necessarily imply the optimal distribution of power among users based on their individual requirements.

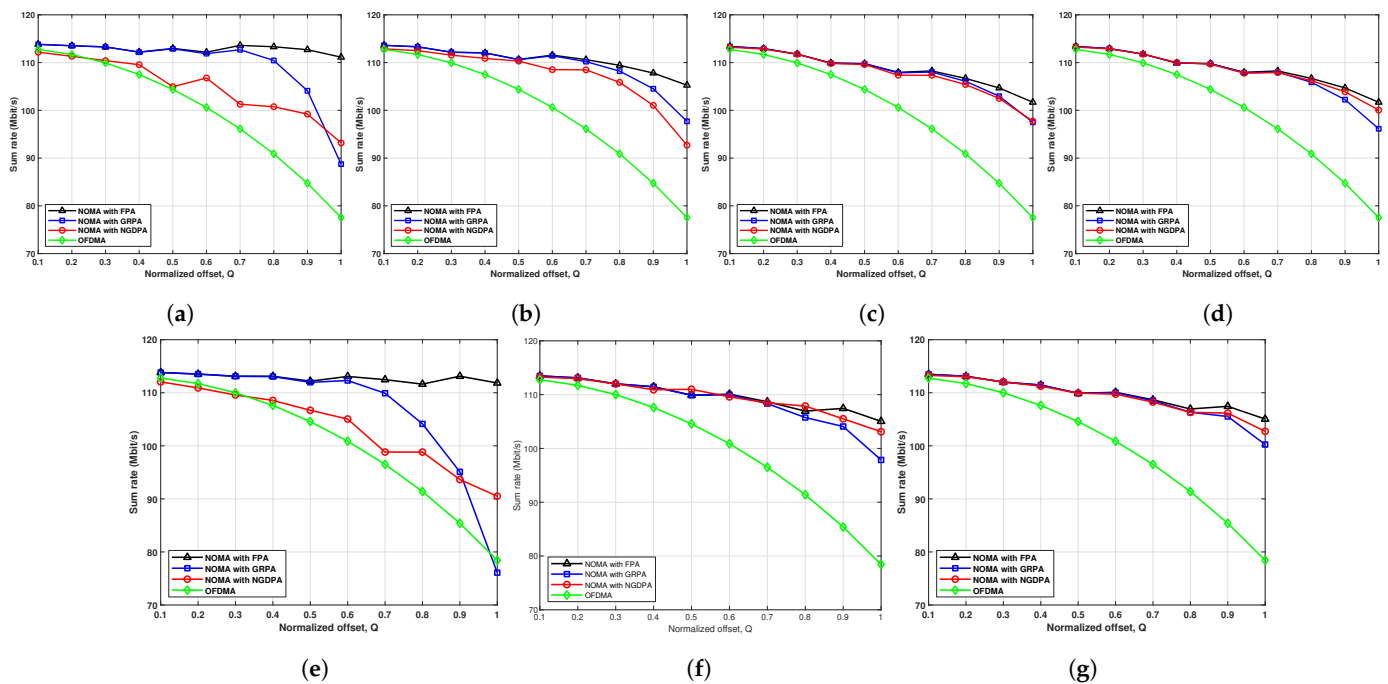


Figure 13. Sum rate vs. normalized offset-based OFDMA and NOMA with five users ($N = 5$) (a) without grouping, (b) using NLUPA/UCGD Strategy 1, (c) NLUPA Strategy 2, (d) UCGD Strategy 2, and six users ($N = 6$) (e) without grouping, (f) using NLUPA and (g) UCGD.

5. Conclusions

In this paper, we explored the performance of two efficient user-pairing algorithms, NLUPA and UCGD, in conjunction with three low-complexity power allocation techniques (FPA, GRPA and NGDPA) in indoor 2×2 MIMO-NOMA VLC systems. The investigation covered achievable rate performance in scenarios with both odd and even numbers of users. The simulation results showed a significant improvement in the achievable rate performance of GRPA with user pairing. Moreover, utilizing user pairing with NGDPA notably reduced instances of users reaching a zero data rate. Furthermore, the findings indicate that NOMA outperforms OFDMA in terms of sum rate. Although FPA achieved the best performance without user grouping, it does not necessarily indicate the optimal distribution of power among users based on their individual requirements.

Author Contributions: Conceptualization, H.S.I. and M.A.; software, H.S.I.; validation, A.M., A.A. and M.A.; writing—original draft preparation, H.S.I.; writing—review and editing, A.M., A.A. and M.A.; supervision, A.M. and A.A. All authors have read and agreed to the published version of the manuscript.

Funding: This research received no external funding.

Institutional Review Board Statement: Not applicable.

Informed Consent Statement: Not applicable.

Data Availability Statement: Data are contained within the article.

Conflicts of Interest: The authors declare no conflict of interest.

References

1. Loureiro, P.A.; Guiomar, F.M.P. Visible Light Communications: A Survey on Recent High-Capacity Demonstrations and Digital Modulation Techniques. *Photonics* **2023**, *10*, 993. [\[CrossRef\]](#)
2. Sadat, H.; Abaza, M.; Mansour, A.; Alfalou, A. A Survey of NOMA for VLC Systems: Research Challenges and Future Trends. *Sensors* **2022**, *22*, 1395. [\[CrossRef\]](#) [\[PubMed\]](#)
3. Jian, Y.H.; Wang, C.C.; Chow, C.W.; Gunawan, W.H.; Wei, T.C.; Liu, Y.; Yeh, C.H. Optical Beam Steerable Orthogonal Frequency Division Multiplexing (OFDM) Non-Orthogonal Multiple Access (NOMA) Visible Light Communication Using Spatial-Light Modulator Based Reconfigurable Intelligent Surface. *IEEE Photonics J.* **2023**, *15*, 1–8. [\[CrossRef\]](#)
4. Ibrahim, H.S.; Abaza, M.; Mansour, A.; Alfalou, A. Power Allocation Techniques for Non-orthogonal Multiple Access Based MIMO Visible Light Communication Systems. In Proceedings of the 2023 8th International Conference on Signal and Image Processing (ICSIP), Wuxi, China, 8–10 July 2023; pp. 930–934. [\[CrossRef\]](#)
5. Abdulwali, J.; Boussakta, S. Visible Light Communication: An Investigation of LED Non-Linearity Effects on VLC Utilising C-OFDM. *Photonics* **2022**, *9*, 192. [\[CrossRef\]](#)
6. Oyewobi, S.S.; Djouani, K.; Kurien, A.M. Visible Light Communications for Internet of Things: Prospects and Approaches, Challenges, Solutions and Future Directions. *Technologies* **2022**, *10*, 28. [\[CrossRef\]](#)
7. Mathur, H.; Deepa, T. A Survey on Advanced Multiple Access Techniques for 5G and Beyond Wireless Communications. *Wirel. Pers. Commun.* **2021**, *118*, 1775–1792. [\[CrossRef\]](#)
8. Alqahtani, A.H.; Almohimmah, E.M.; Alresheedi, M.T.; Abas, A.F.; Qidan, A.A.; Elmirghani, J. Decoding-Order-Based Power Allocation (DOPA) Scheme for Non-Orthogonal Multiple Access (NOMA) Visible Light Communication Systems. *Photonics* **2022**, *9*, 718. [\[CrossRef\]](#)
9. Saxena, P.; Chung, Y.H. Performance analysis of a NOMA-VLC system with random user location. *ICT Express* **2023**, *9*, 439–445. [\[CrossRef\]](#)
10. Mohsan, S.A.H.; Sadiq, M.; Li, Y.; Shvetsov, A.V.; Shvetsova, S.V.; Shafiq, M. NOMA-Based VLC Systems: A Comprehensive Review. *Sensors* **2023**, *23*, 2960. [\[CrossRef\]](#)
11. Bawazir, S.S.; Sofotasios, P.C.; Muhaidat, S.; Al-Hammadi, Y.; Karagiannidis, G.K. Multiple Access for Visible Light Communications: Research Challenges and Future Trends. *IEEE Access* **2018**, *6*, 26167–26174. [\[CrossRef\]](#)
12. Li, Y.T.; Geng, T.W.; Gao, S.J. On the signal combinations for a uniquely decodable coded MIMO-FSO communication system. *Opt. Laser Technol.* **2024**, *172*, 110533. [\[CrossRef\]](#)
13. Lin, B.; Ghassemlooy, Z.; Tang, X.; Li, Y.; Zhang, M. Experimental demonstration of optical MIMO NOMA-VLC with single carrier transmission. *Opt. Commun.* **2017**, *402*, 52–55. [\[CrossRef\]](#)
14. Li, Q.; Shang, T.; Tang, T.; Dong, Z. Optimal Power Allocation Scheme Based on Multi-Factor Control in Indoor NOMA-VLC Systems. *IEEE Access* **2019**, *7*, 82878–82887. [\[CrossRef\]](#)
15. Marshoud, H.; Kapinas, V.M.; Karagiannidis, G.K.; Muhaidat, S. Non-Orthogonal Multiple Access for Visible Light Communications. *IEEE Photonics Technol. Lett.* **2016**, *28*, 51–54. [\[CrossRef\]](#)
16. Chen, C.; Zhong, W.D.; Yang, H.; Du, P. On the Performance of MIMO-NOMA-Based Visible Light Communication Systems. *IEEE Photonics Technol. Lett.* **2018**, *30*, 307–310. [\[CrossRef\]](#)
17. Zhu, L.; Zhang, J.; Xiao, Z.; Cao, X.; Wu, D.O. Optimal User Pairing for Downlink Non-Orthogonal Multiple Access (NOMA). *IEEE Wirel. Commun. Lett.* **2019**, *8*, 328–331. [\[CrossRef\]](#)
18. Han, Y.; Zhou, X.; Yang, L.; Li, S. A Bipartite Matching Based User Pairing Scheme for Hybrid VLC-RF NOMA Systems. In Proceedings of the 2018 International Conference on Computing, Networking and Communications (ICNC), Maui, HI, USA, 5–8 March 2018; pp. 480–485. [\[CrossRef\]](#)
19. You, H.; Pan, Z.; Liu, N.; You, X. User Clustering Scheme for Downlink Hybrid NOMA Systems Based on Genetic Algorithm. *IEEE Access* **2020**, *8*, 129461–129468. [\[CrossRef\]](#)
20. Ding, Z.; Fan, P.; Poor, H.V. Impact of User Pairing on 5G Nonorthogonal Multiple-Access Downlink Transmissions. *IEEE Trans. Veh. Technol.* **2016**, *65*, 6010–6023. [\[CrossRef\]](#)
21. Shahab, M.B.; Irfan, M.; Kader, M.F.; Shin, S. User Pairing Schemes for Capacity Maximization in Non-orthogonal Multiple Access Systems. *Wirel. Commun. Mob. Comput.* **2016**, *16*, 2884–2894. [\[CrossRef\]](#)
22. Marshoud, H.; Sofotasios, P.C.; Muhaidat, S.; Karagiannidis, G.K.; Sharif, B.S. On the Performance of Visible Light Communication Systems With Non-Orthogonal Multiple Access. *IEEE Trans. Wirel. Commun.* **2017**, *16*, 6350–6364. [\[CrossRef\]](#)

23. Komine, T.; Nakagawa, M. Fundamental analysis for visible-light communication system using LED lights. *IEEE Trans. Consum. Electron.* **2004**, *50*, 100–107. [[CrossRef](#)]
24. Yin, L.; Popoola, W.O.; Wu, X.; Haas, H. Performance Evaluation of Non-Orthogonal Multiple Access in Visible Light Communication. *IEEE Trans. Commun.* **2016**, *64*, 5162–5175. [[CrossRef](#)]

Disclaimer/Publisher’s Note: The statements, opinions and data contained in all publications are solely those of the individual author(s) and contributor(s) and not of MDPI and/or the editor(s). MDPI and/or the editor(s) disclaim responsibility for any injury to people or property resulting from any ideas, methods, instructions or products referred to in the content.